

Retraction

Retracted: Content-Based Image Retrieval Using Gamma Distribution and Mixture Model

Journal of Function Spaces

Received 23 January 2024; Accepted 23 January 2024; Published 24 January 2024

Copyright © 2024 Journal of Function Spaces. This is an open access article distributed under the Creative Commons Attribution License, which permits unrestricted use, distribution, and reproduction in any medium, provided the original work is properly cited.

This article has been retracted by Hindawi following an investigation undertaken by the publisher [1]. This investigation has uncovered evidence of one or more of the following indicators of systematic manipulation of the publication process:

- (1) Discrepancies in scope
- (2) Discrepancies in the description of the research reported
- (3) Discrepancies between the availability of data and the research described
- (4) Inappropriate citations
- (5) Incoherent, meaningless and/or irrelevant content included in the article
- (6) Manipulated or compromised peer review

The presence of these indicators undermines our confidence in the integrity of the article's content and we cannot, therefore, vouch for its reliability. Please note that this notice is intended solely to alert readers that the content of this article is unreliable. We have not investigated whether authors were aware of or involved in the systematic manipulation of the publication process.

Wiley and Hindawi regrets that the usual quality checks did not identify these issues before publication and have since put additional measures in place to safeguard research integrity.

We wish to credit our own Research Integrity and Research Publishing teams and anonymous and named external researchers and research integrity experts for contributing to this investigation.

The corresponding author, as the representative of all authors, has been given the opportunity to register their agreement or disagreement to this retraction. We have kept a record of any response received.

References

- [1] Y. D. Khan, M. K. Mahmood, D. Ahmad, and N. M. Al-Zidi, "Content-Based Image Retrieval Using Gamma Distribution and Mixture Model," *Journal of Function Spaces*, vol. 2022, Article ID 8674038, 10 pages, 2022.

Research Article

Content-Based Image Retrieval Using Gamma Distribution and Mixture Model

Yaser Daanial Khan ¹, M. Khalid Mahmood ², Daud Ahmad ², and Nasser M. Al-Zidi ³

¹School of Systems and Technology, University of Management and Technology Lahore, Pakistan

²Department of Mathematics, University of the Punjab, Lahore, Pakistan

³Faculty of Administrative and Computer Sciences, Albaydha University, Albaydha, Yemen

Correspondence should be addressed to Nasser M. Al-Zidi; alzidi.nasser@baydaauniv.net

Received 3 March 2022; Accepted 9 April 2022; Published 5 May 2022

Academic Editor: Muhammad Gulzar

Copyright © 2022 Yaser Daanial Khan et al. This is an open access article distributed under the Creative Commons Attribution License, which permits unrestricted use, distribution, and reproduction in any medium, provided the original work is properly cited.

Since the last decade, the complexity of multimedia data, specifically images, is emerging exponentially as millions of images are uploaded by users on daily basis. Searching for a relevant image from such a substantial amount of data is very hectic and resource-demanding. To cope with this issue, researchers are working on content-based image retrieval (CBIR) approaches. This article proposes an efficient and novel probabilistic technique as a solution for content-based image retrieval. The patterns formed by the glyph structure of an image are excavated to yield content representations. These representations are accumulatively used to form a distribution, whereas the characteristics of this distribution represent the semantic structure of the image. In the end, the mixture model for gamma distribution is applied and parameters are refined through maximum likelihood. Furthermore, a mechanism is devised to retrieve matching images having comparable distribution patterns. Experiments show not only that the proposed technique yields a comparable precision to other competitive techniques but it also demonstrates that it is sufficiently efficient with high performance compared as compared to the others and requires unsupervised training.

1. Introduction

The effortless availability of multimedia documents and related devices has significantly increased the essential needfulness of image indexing and searching techniques. Researchers have designed and habituated various algorithms for this purpose [1–3]. A versatile algorithm usually provides appropriate parametrization for the purpose of broadening and/or narrowing down the result set. The simplest technique used for obtaining images on the basis of its contents is the use of footnotes. In such a scheme, images persist along with their textual description which enables an application to retrieve images based on some textual criterion [4–8]. At times, this technique fails to produce formative results, as text may not truly describe an image. Textual criterion and description should be substituted by images to provide a more accurate depiction [9–12]. This calls for the need of image processing and

computer vision techniques to be employed. Also, various stochastic, intelligent, and/or probabilistic techniques are used for the extraction of patterns within an image [13]. The extracted patterns are described in terms of a number of parameters which are equated to find a match within an acceptable range of error [14–18].

A number of approaches used to solve the described problem are found in the literature [19–21]. Some authors have extracted the semantic information within images and fed it into some probabilistic model to obtain parametric description of images [22, 23]. The extracted information typically represents the normalized pixel values in a compressed form signifying the image semantics [24–27].

Jiang et al. [28] propose a feature vector using the visually interesting information in the image. These feature vectors are statistically analyzed to produce some results. Wu and Yap [29] have used support vector machine (SVM) for the purpose. Each image is used as labeled data, and fuzzy

logic is employed to classify the label for each image. SVM is trained using these labels, and after sufficient training, the SVM is able to retrieve images on the basis of its contents. Neural network (NN) is a nonparametric statistical model while it has also been used for the proposed problem. Information hidden within the images is fed into a NN to analyze and to match images [30].

Various relevance feedback-based methods have been devised by researchers. Feedback from a number of users is collected about the contents of the image. Using this feedback, the correlation capability and feature identification capability are developed iteratively [31, 32]. In order to produce assiduous results, it is essential to take an image as a whole and not just consider its partial features [33]. Most of the techniques discussed earlier focus on localized features of an image. Some of the techniques which use NN or SVM require a training process which sometimes proves to be time taking and convoluted [34]. Moreover, it fails to provide formative results if the training data is small or localized while the test data is disproportionately large and globalized [35]. In case the training data is diversified, then its huge size renders the training process to be more formidable [36].

Besides machine learning, various methods have been proposed based on deep neural networks. Rao et al. in 2021 proposed a deep learning-based architecture for content-based image retrieval using convolution-based stacks to compute image representations [37]. Similarly, in 2021, Singh et al. proposed a method using deep convolutional networks for large facial datasets [38]. In 2019, Saritha et al. proposed a deep belief network-based approach to perform efficient image retrieval [39]. The authors used the DBN for the computation of deep representations of images and their classification. Similarly, in 2019, Sharif et al. proposed a method relying on binary robust invariant scalable keypoints and scale-invariant feature transform [40]. SIFT was observed to perform well even with the presence of noise, rotation, and variance in good light conditions; however, with low light conditions, it did not perform well. But by the fusion of binary robust invariant scalable keypoints, this issue was resolved. Tzelepi and Tefas, in 2018, proposed a convolutional neural network-based model for content-based image retrieval [41, 42]. However, all of these methods work on basically large datasets and require extensive computations for the training of models, as they work on the principles of supervised learning.

In this article, we provide a globalized approach for the problem. Furthermore, the training process bears insignificant computational overheads. This approach treats an image as a whole and appreciates all its contents. All the features of an image impact upon the quantification of attributes of data pattern presented by an image. These attributes hence generated are used to find a match within an acceptable range of error. Moreover, the size of the attributes extracted is trifling, and this fact makes the proposed model most appropriate for searching and indexing services. The paper is organized as follows. Section 2 discusses the methods comprising preprocessing for the feature extraction of images, coding and glyph structures, details of probabilistic model proposed in this article, parameters obtained, and

their refinement by applying the principle of maximum likelihood. Main results and their analysis are provided in Section 3. The article concludes with Section 4 with some discussion and conclusions.

2. Methods

The flowchart of the study is shown in Figure 1.

2.1. Preprocessing for Feature Extraction. A number of preprocessing steps must be performed before semantically significant features from the image are extracted. Typically, an image contains noise which hampers extraction of edges and contours. Median filtering [28] is applied to eradicate sporadic salt and pepper noise from the image result is shown in Figure 2(b). Secondly, the image is blurred to produce an image as shown in Figure 2(c). In the next step, Canny edge detection algorithm is applied to sieve out the edges as shown in Figure 2(d). Notice the edges in Figure 2(d), forming a glyph-like pattern. Hence, we term it as the glyph structure of the image. It is also noticed that some of the glyphs are long and stretched while some are short. We shall treat each glyph as component of the image and encode the data embedded within them to find useful patterns.

2.2. Coding the Glyph Structure. In Section 2, a glyph structure from an image was isolated. In this section, each glyph is extracted from the image and encoded in an appropriate way. The method adopted for encoding each glyph is chain code. Chain code is a compendious method for depicting a number of points on a plane which are connected to each other. It provides a concise method for developing a numeric code rather than enlisting Cartesian coordinates for a set of connected points [43]. The eight connected grid is exploited to form the chain code which signifies that each pixel has eight neighboring pixel. The code is formed by tracing along the thinned glyph. Figure 3 shows the code assigned to each neighboring pixel. The East pixel is coded 0, and subsequently, the code is incremented on each 45-degree step in anticlockwise direction. Next, digit in the code is assigned depending upon the phase of the next neighboring pixel. Figure 4 shows a thinned glyph along with its chain code. The major advantage of this code is its translation invariant. The location information for each glyph has been omitted, and only the information pertaining to relative positioning of pixels has been retained. Moreover, the derivative of chain code exhibits rotation invariant properties. The probability density function proposed in this paper makes no use of the length metrics of the glyph; hence, the disadvantage posed by chain code along diagonal transition has no effect on the proposed model.

2.3. Use of Probabilistic Techniques. High-resolution images encompass large amount of raw data which needs to be transformed into a succinct form in order to reduce computational overhead. The model in turn outputs a set of parameters or a feature vector which is used as a numeric quantification of semantic characteristics of data. Similar attributes are extracted using data patterns hidden within an image. These attributes empower to establish whether

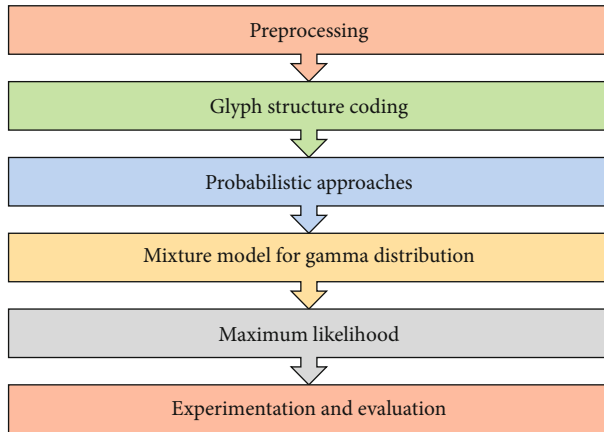


FIGURE 1: Flowchart of the proposed method.

an arbitrary image matches another criterion image or not. In the proposed work, mixture model (MM) is used for the same purpose. A MM combines various independent random variable components yielding a mixture distribution. In a MM, each independent variable imparts a fractional impact [14, 19–21]. Each glyph forms an independent variable of the mixture while the image is a paradigm of glyphs. The data extorted out of each glyph needs to be jibed into a probability density function. This issue is resolved coercing the code chain of each glyph into a histogram. As eight connected grid has been used, therefore, the histogram has eight different bins. The frequency of occurrence of each connected element in a glyph is tabulated, and hence, a probability distribution is formed using the gamma distribution [44]. Each glyph component is represented by the parameters yielded from its data. The main advantage of mixture models is that it incorporates the parameters of each component to form comprehensive parameter. Furthermore, estimation techniques like maximum likelihood are applied on mixtures to converge the parameters to their optimal.

Mixture models are used as an interesting statistical tool. They are used to extract information from data if the data is of hierarchical nature. This probabilistic model is used to impart significance of groups within a population. Mixture models may not essentially require the identity of the group to which a dataset belongs. The choice of distribution function being incorporated into the mixture model depends upon the nature of data. In the proposed work, the distribution used is the gamma distribution because many random variables are special cases of the gamma random variable. Further, by varying the shape and the rate parameter, it is possible to fit the gamma probability density function into many types of experimental data. Since the gamma distribution is skewed in any direction, therefore, the major dividend the gamma distribution presents is that it has the capability to accommodate randomly distributed data in any direction [44]. The proposed work presents a concrete model for the glyph structure of an image. Subsequently, an arbitrary glyph may have shapes varying from regular ones to haphazard ones; hence, gamma distribution forms a suitable framework to model arbitrary glyphs.

Gamma distribution belongs to the class of distributions having two parameters. These parameters are denoted as k and θ where k is called the shape parameter and θ is called the scale parameter.

Equivalently, some text also refers gamma distribution to have parameters α and β where $k = \alpha$ but β is the inverse scale parameter and is given as $\beta = 1/\theta$ also called the rate parameter. Suppose a random variable X exhibits gamma distribution, then the following notation is used in terms for k and θ is used to define X , where $X \sim \Gamma(k, \theta) = \text{gamma}(k, \theta)$. The gamma probability density function using shape and scale parameters is given as

$$f(x; k, \theta) = \frac{x^{k-1} e^{-x/\theta}}{\theta^k \Gamma(k)}, \quad (1)$$

where $x > 0$ and also $k, \theta > 0$. The similar function for shape and rate parameters is given as

$$f(x; \alpha, \beta) = \frac{\beta^\alpha x^{\alpha-1} e^{-\beta x}}{\Gamma(\alpha)}, \quad (2)$$

where $x > 0$ and also $k, \theta > 0$. Also, $\Gamma(x)$ is the gamma function given as

$$\Gamma(x) = \int_0^\infty t^{x-1} e^{-t} dt. \quad (3)$$

A glyph tracing algorithm is developed to scan and quantify glyphs in a crisp form. The filtered image is scanned left to right and top down, to search for glyphs. On encountering a glyph, it traces through adjacent pixels to find the starting end point closer to the top left point of the image. Now beginning from this, start point the algorithm traverses through each pixel of the glyph until it reaches the next end point. On traversing each pixel, the chain code for the glyph is updated in accordance with the direction of the pixel. A histogram is formed from the chain code of each glyph. This histogram is now jibed into the gamma distribution to obtain distribution parameters.

2.4. Adopting the Mixture Model for Gamma Distribution Using Glyph Structure. In this section, a method is designated for incorporating the parameters generated in the previous section into the mixture model adapted for gamma distribution function. Let each glyph within the image correspond to gamma distribution random variable given as $\{X_1, X_2, \dots, X_m\}$ while there are m glyphs in the image. As described in Section 2.3, the parameters describing each glyph are individually computed and let those be given as $\{\alpha_1, \alpha_2, \dots, \alpha_m\}$, $\{\beta_1, \beta_2, \dots, \beta_m\}$. Each glyph component is coerced into the gamma distribution yielding parameters α_i and β_i . The density of the i^{th} component within the image is described by the distribution function given below:

$$f_i(x_i; \alpha_i, \beta_i) = \frac{\beta_i^{\alpha_i} x_i^{\alpha_i-1} e^{-\beta_i x_i}}{\Gamma(\alpha_i)}, \quad (4)$$



FIGURE 2: From raw image to edge detection: (a) Raw image, (b) image after grey-scale conversion, (c) blurring after median filtering, and (d) edges extracted from the image.

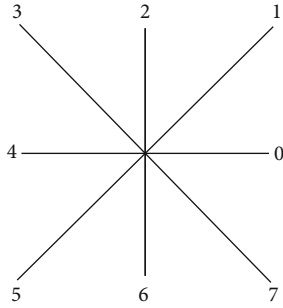


FIGURE 3: Values assigned to each neighboring pixel in the signified direction in an 8-connected grid.

where x^{α_i-1} represents distribution variables, and gamma distribution parameters are $\beta_i^{\alpha_i}$ and α_i . The mixture model assigns weight to each component for its proportional incorporation into the whole mixture. Usually, initial weights are assigned randomly but here, we impart a weight to each glyph in accordance with its size. Weight assigned to each glyph is the ratio of the number of pixels along the glyph and total number of pixel along each glyph within the image. Let g_i denote the set of points within the i^{th} glyph; then, its initial weight b_i is given as follows:

$$b_i = \frac{|g_i|}{\sum_{k=1}^m |g_k|}, \quad (5)$$

where $|g_i|$ represents number of pixels along the glyph, and total number of pixel along each glyph within the image is $\sum_{k=1}^m |g_k|$. In the previous steps, the probability density for individual glyphs and their initial weights are calculated. In the next step, using the probability density of glyphs and their weight, the probability density of the mixture and hence its parameters are calculated [19–21]. The mixture probability density is given as

$$F_j(x) = \sum_{k=1}^m b_k f_k(x). \quad (6)$$

Expanding Equation (4) into Equation (6), we get

$$F_k(x) = \sum_{k=1}^m b_k f_k(x; \alpha_k, \beta_k) = \sum_{k=1}^m \frac{b_k \beta_k^{\alpha_k} x^{\alpha_k-1} e^{-\beta_k x}}{\Gamma(\alpha_k)}. \quad (7)$$

The mixture probability density function, given in Equation (7), is used to generate its parameters. However, at the moment, these values are raw and should be processed to obtain optimal value. Maximum likelihood algorithm is used to converge these values to the optimal as explained in the following section.

2.5. Applying Maximum Likelihood. The actual distribution of data in any model is random in nature. The acquired samples are fitted onto a distribution, and it is assumed that it will abide by a certain distribution function depending on the size, occurrence, and nature of data. In the previous section, it was assumed that the data abides by gamma distribution. Based on this assumption, the data is entirely and thoroughly homologized into gamma mixture model. The collected samples do not truly represent the whole population. Maximum likelihood algorithm is used to estimate the hidden or inaccessible data and subsequently improve the distribution parameters [7, 13]. More simply, maximum likelihood enables us to adjust the parameters of the distribution such that it forms a closer alignment with gamma distribution at each step. Let x_1, x_2, \dots, x_m be the samples forming the population within distribution; then, the likelihood function of these random samples is given as follows:

$$L(\theta) = f(x_1, x_2, \dots, x_m; \theta). \quad (8)$$

Let these random samples correspond to random variables such that x_1 corresponds to X_1 and x_2 corresponds to X_2 . Since each of the variable is independent, therefore,

$$L(\theta) = f(x_1, \theta) \cdot f(x_2, \theta) \cdots f(x_m, \theta), \quad (9)$$

or

$$L(\theta) = \prod_{i=1}^m f(x_i, \theta). \quad (10)$$

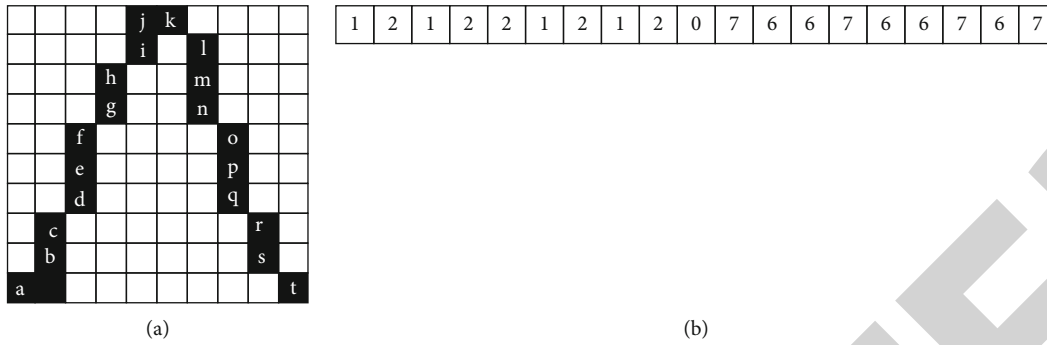


FIGURE 4: Glyph representation. (a) A glyph component with pixels labeled a, b, c, \dots, t . (b) The chain code representation of the glyph.

Now we take the log-likelihood, and after simplification, it yields

$$l(k, \theta) = (k-1) \sum_{i=1}^N \ln(x_i) - Nk - Nk \ln\left(\frac{\sum x_i}{kN}\right) - N \ln(\Gamma(k)). \quad (11)$$

Taking the partial derivative $\partial l / \partial \theta$ and solving it by putting it equal to zero using maximum likelihood principle, we get the improved θ given as

$$\theta = \frac{1}{kN} \sum_{i=1}^N x_i. \quad (12)$$

Now substituting this value of θ , Equation (12) into Equation (11), we get

$$l = (k-1) \sum_{i=1}^N \ln(x_i) - Nk - Nk \ln\left(\frac{\sum x_i}{kN}\right) - N \ln(\Gamma(k)). \quad (13)$$

Again in accordance with the principle of maximum likelihood taking the derivative of Equation (13), after eliminating θ , with respect to k and putting it equal to zero, we get

$$\ln(k) - \psi(k) = \ln\left(\frac{1}{N} \sum_{i=1}^N x_i\right) - \frac{1}{N} \sum_{i=1}^N \ln(x_i), \quad (14)$$

where ψ is called the gamma function and is given by the following.

$$\psi(x) = \frac{\Gamma'(x)}{\Gamma(x)}. \quad (15)$$

Using some careful approximations, it has been proved in [45] that

$$\ln(k) - \psi(k) \approx \frac{1}{2k} \left[1 + \frac{1}{6k+1} \right]. \quad (16)$$

Moreover, after applying Newton-Raphson for numerical estimation of k , we get

$$k = k - \frac{\ln(k) - \psi(k) - s}{1/k - \psi'(k)}. \quad (17)$$

The above described process yields improved parameters. This process is repeated until convergence is achieved which means that there is no appreciable change in parameters within successive iterations.

3. Experiments and Results

A large database of images was compiled constituting images of varying resolution. The multitude of images exhibited diversity in terms of the semantic contents. The glyph structure was filtered out for each image and for each glyph in the image a chain code was formed. The chain code was used to form a histogram and hence its distributions function. The parameters of the distribution achieved for an image were homologized in a mixture. Furthermore, the yielded parameters of the mixture are further refined until they converged using maximum likelihood. Ultimately, the parameters of the mixture model achieved after convergence represented the characteristics of the image. Comparison among various images is established by dealing out with their corresponding parameters. As result of several experiments carried out and discussed later, it is deduced that parameters of semantically nonresembling images differ while semantically resembling images have comparable parameters.

3.1. Experiment 1. A comparison criterion is established based on the kurtosis and skewness of the mixture distribution obtained for an image. The kurtosis tells us about the height of the distribution while skewness signifies the extent by which the distribution leans away from the mean. Arbitrary distribution with comparable skewness and kurtosis measures is likely to have approaching shape and other characteristics. The skewness measure of gamma distribution for an arbitrary i^{th} image is given as

$$S_i = \frac{2}{\sqrt{k_i}} \text{ or } S_i = \frac{2}{\sqrt{\alpha_i}}, \quad (18)$$

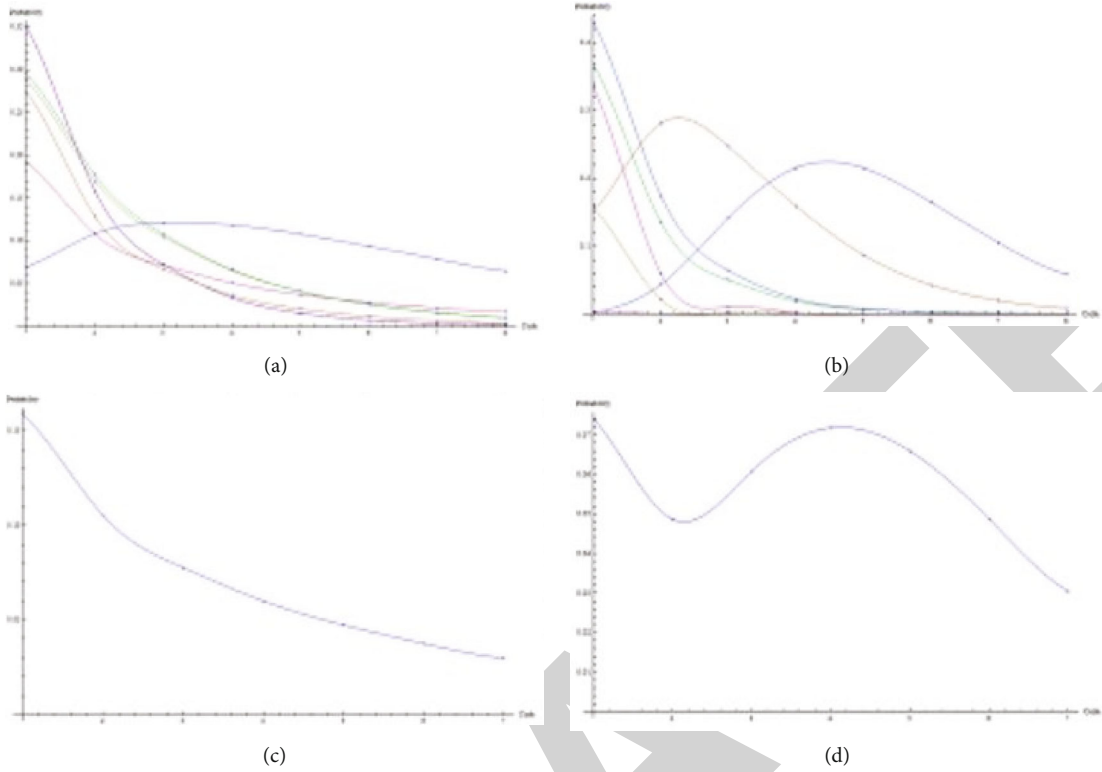


FIGURE 5: (a, b) Distribution patterns and mixtures of each of the component glyphs and (c, d) the mixtures obtained for (a, b), respectively.

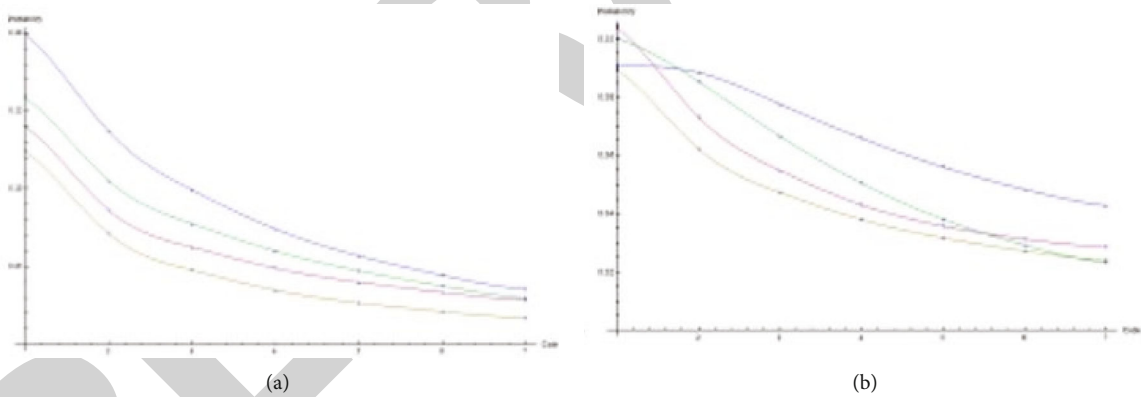


FIGURE 6: Result of maximum likelihood. (a) Mixture distribution for four different images. (b) After few iterations of maximum likelihood.

while the kurtosis [44] is measured as

$$U_i = \frac{6}{k_i} \text{ or } U_i = \frac{6}{\alpha_i}. \quad (19)$$

Euclidean distance among the features of arbitrary mixtures attained for arbitrary images is used as the criterion for finding matches. It is computed using the following equation:

$$D = \sqrt{(U_i - U_k)^2 + (K_i - K_j)^2}. \quad (20)$$

Figures 5(a) and 5(b) show gamma distributions obtained for the glyph structure of two matching images

while Figures 5(c) and 5(d) show the distribution of the mixtures obtained for the same pair of images. Note that both the mixture distributions resemble each other in shape. Moreover, Figure 6(a) shows gamma mixture distribution of various resembling images while Figure 6(b) shows the same distributions after few iterations of maximum likelihood. Note that either the distributions have converged or diverged from each other. This shows the significance of maximum likelihood process. It helps to make resemblance or dissimilarity among distribution patterns more apparent. Furthermore, Figure 7(a) shows the mixture distribution pattern for two resembling images while Figure 7(b) shows the pattern for two moderately dissimilar images. The Euclidean distance is used to devise a mechanism for exploiting the similarity or dissimilarity of distribution

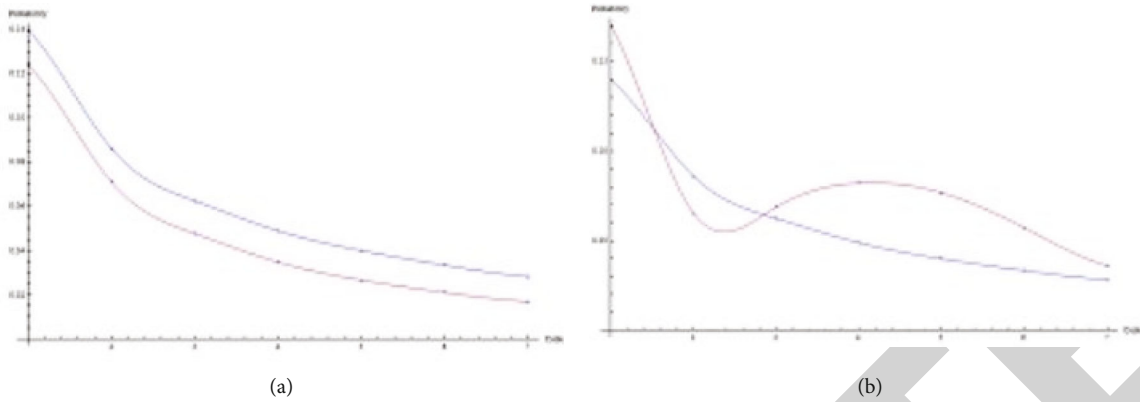


FIGURE 7: Mixture distributions for (a) resembling images and (b) unlike images.

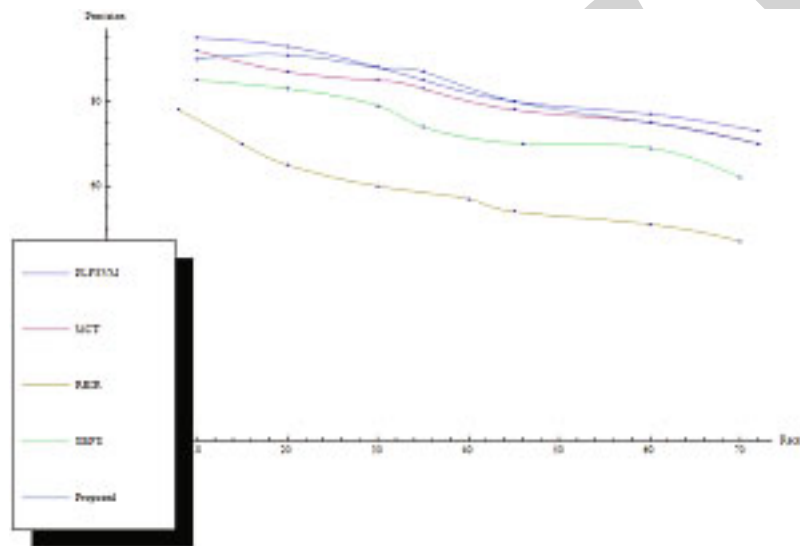


FIGURE 8: Precision-recall graph for certain competitive techniques in comparison with the proposed one.

shapes. The distance measure elucidates whether a target image is a match or not.

3.2. *Experiment 2.* In this experiment, certain metrics are realized as a benchmark illustrating the accuracy of the proposed model. Precision-recall is an interesting accuracy measure. The precision is the measure of retrieved instances which were relevant to the search criteria while recall is the measure of relevant images that were retrieved. A precision-recall graph is a useful graphical depiction for such models. It is used to summarize the performance of a system in terms of accuracy. Precision and recall data was collected for various existing competitive models along with the proposed model. A region-based image retrieval model (RBIR) firstly segments an image and then extracts feature vectors from each segment. A dissimilarity function is used to calculate the distance between two arbitrary segments and output a result [46]. In another approach [47], the authors segment an image and perform multiresolution analysis using three measures, namely, the color autocorrelogram, block variation of local correlation coefficients (BVLC), and block difference of inverse probabilities (BDIP). An image is also

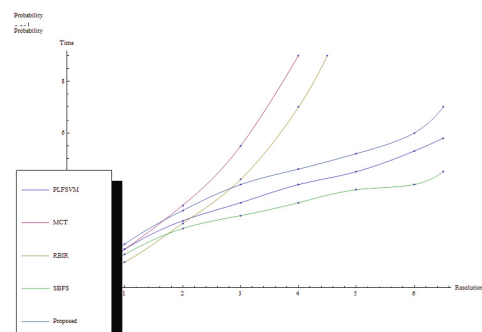


FIGURE 9: Performance of the proposed approach and other competitive techniques.

decomposed into various segments in [28]. Principal component analysis (PCA) is used to decompose a segment into a small feature space. A saliency membership is used to correlate a segment with an image. In [29], a pseudo labeled fuzzy vector machine is employed for the purpose. A fuzzy membership function is defined to estimate the class association of an image. This function is further used

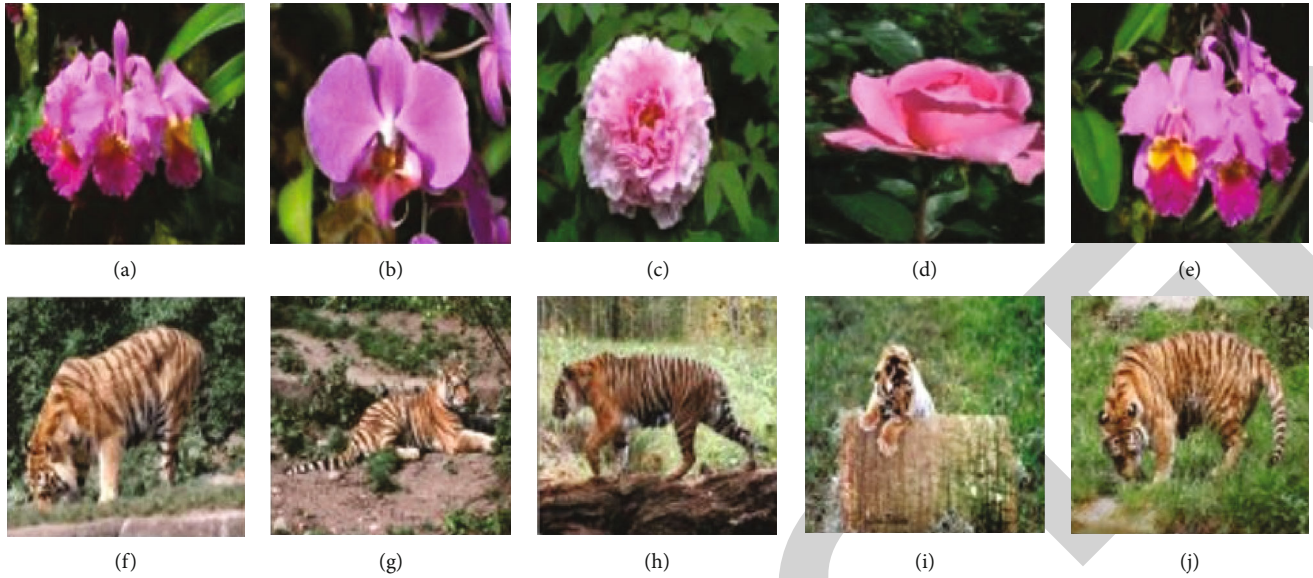


FIGURE 10: Generated results through proposed approach. (a) Original image, (b–e) retrieved images when (a) is given as criterion image, (f) original image, and (g–j) retrieved images where (f) is used as criterion.

to train the SVM. The compiled database is tested for each of the described current state of the art methods along with the proposed one. The performance of each model is illustrated using a precision-recall graph as shown in Figure 8.

3.3. Experiment 3. In order to realize the efficiency of each discussed technique, the underlying experiment is conducted. All the images in the database were sorted in ascending order based on their resolution. The time taken by each of the technique, discussed in experiment 2, was observed for each image. The graph shown in Figure 9 was plotted which showed the increase in running time of each algorithm as the resolution of the image is increased. Further, Figure 2 shows some of the images retrieved for different queries. In the first query, the image in Figure 10(a) was given as criteria while Figures 10(b)–10(e) show some of the retrieved results. In another query, the image in Figure 10(f) was given as criterion and images in Figures 10(g)–10(j) were retrieved.

3.4. Discussion. In experiment 1, the performance was evaluated by using skewness and kurtosis measures. Later, a pair of two similar images was used for glyph structure extraction and analysis of their gamma distribution of mixtures. It was observed that both distributions resembled cases of similar images. Later, to show the process of refinement through maximum likelihood, a few iterations were applied and it was observed that the distributions converged/diverged after refinement. Lastly, to observe the behaviour of the proposed algorithm for similar images in comparison with unlike images, the whole process was applied to a pair of similar images and a pair of unlike images, whereas to compute the difference in distributions, Euclidean distance was used. The results were observed to be accurate in terms of both

similar images and unlike images, as distributions were in harmony for similar images.

For the second experiment, precision-recall curves were plotted in comparison with other well-known state-of-the-art approaches, and it was observed that the proposed method outperformed the others in terms of precision and recall, which represents higher preciseness and accuracy for correct image retrieval by the proposed algorithm.

Lastly, to test the image retrieval efficiency of the proposed algorithm, the whole database of images was used and a query was made using different images to see whether our proposed algorithm efficiently retrieves the relevant images or not. The efficiency was computed in terms of running time, and it was observed that the proposed method outperformed the others in terms of efficiency as well.

4. Conclusions

The major motivation behind the development of this model was the need to devise an image-based search engine or indexing service. The proposed model was implemented through persistence of the mixture model parameters and few of its moments for an image in conjunction with the location of the image. A user submits his search criterion in form of another image. The features of the criterion image are computed and compared with those already persisting within the indexing service to find possible matches. At times, the result set is extremely large or extremely small. Some extended measure needs to be taken in order to reduce or expand the result set in such cases. A threshold distance is defined for this purpose. It signifies the range of Euclidean distance between the criterion image features and target image features within which the target image is marked as a match. This allows the user to expand or contract the result set by changing the threshold.

After analysis of all the images in the database and their respective parameters, kurtosis, and skewness measures, the following inferences were collected.

- (1) In case two images match semantically, then their features (parameters, kurtosis, and skewness) will also match. Identical images will have identical parameters while the features of resembling images are comparable
- (2) The corresponding features will greatly deviate from each other if both the images are semantically far apart
- (3) In arbitrary images, arbitrary glyphs which may not seem to be identical may form resemblance after being coerced into gamma distribution
- (4) Some of the results suggest that the technique is probabilistic in nature as some of the images acquired comparable parameters even though they seemed semantically different

Most of the systems proposed by other authors focus on localized characteristics of an image whereas the proposed model uses the global features of an image. The global characteristics of an image are quantified into numerical features. The essence of the technique lies in the translation of an image into a probability density function. The model uses data obtained through chain code encoding of glyph structure. As discussed earlier, the chain code data is translation invariant as it keeps no track of glyph location. Also, once a glyph is transformed into a probability density function, the parametric representation of a glyph is scale invariant. A glyph of the same shape scaled up or down yields the same or comparable features. This theoretical perception is substantiated by practical results. The results obtained also show that the technique is scale and translation invariant. It is able to identify the similarity between two arbitrary images even though the sizes of the images are different. Similar phenomenon is observed even if the location of corresponding objects within the images differs. Both the facts imply that the model is scale and translation invariant.

Several steps need to be performed on an image in order to extract its sumptuous parameters. The process starts on a raw image which is initially passed through several filters to remove noise and extract edges. The edges are discretely extracted and encoded using 8-connected chain codes. The parameters obtained from each glyph are used to yield parameters of the mixture. This processing of image from the start till end is at large computationally intensive for high-resolution images. However, efficient algorithms and sufficiently fast hardware certainly reduce the computational time involved. This property of the algorithm makes it most appropriate for searching and indexing applications working off-line. Figure 9 shows the efficiency of this technique in comparison with other such techniques. It is observed that the proposed technique performs sufficiently well over others especially over the techniques which use multiresolution analysis or some transformations. In addition, from Figure 8, it is observed that the proposed technique provides

a precision gain over other and its performance is quite comparable to PLFSVM technique. On the other hand, PLFSVM requires extensive supervised training and initial semantic labeling of samples while in the proposed technique, few computations are required to achieve convergence through maximum likelihood method.

Data Availability

No data were used to support this study.

Conflicts of Interest

The authors of the manuscript are herewith confirm that they have no conflict of interest of this research article.

References

- [1] J. Canny, "A computational approach to edge detection," *Institute of Electrical and Electronics Engineers Transactions on Pattern Analysis and Machine Intelligence*, vol. PAMI-8, no. 6, pp. 679–698, 1986.
- [2] R. Deriche, "Using Canny's criteria to derive a recursively implemented optimal edge detector," *The International Journal of Computer Vision*, vol. 1, no. 2, pp. 167–187, 1987.
- [3] A. P. Dempster, N. M. Laird, and D. B. Rubin, "Maximum likelihood from incomplete data via the EM algorithm," *Journal of the Royal Statistical Society, Series B*, vol. 39, no. 1, pp. 1–22, 1977.
- [4] R. V. Hogg, J. W. McKean, and A. T. Craig, *Introduction to Mathematical Statistics*, Pearson Education, 2005.
- [5] D. J. MacKay, *Information Theory, Inference and Learning Algorithms*, Cambridge University Press, 2003.
- [6] J. A. Bilmes, *A Gentle Tutorial of the EM Algorithm and Its Application to Parameter Estimation for Gaussian Mixture and Hidden Markov Models*, International Computer Science Institute, 1998.
- [7] T. K. Moon, "The expectation-maximization algorithm," *IEEE Signal Processing Magazine*, vol. 13, no. 6, pp. 47–60, 1996.
- [8] T. K. Nasios and A. G. Bors, "Variational learning for Gaussian mixture models," *IEEE Transactions on Systems, Man and Cybernetics, Part B*, vol. 36, no. 4, pp. 849–862, 2006.
- [9] Y. V. Venkatesh, S. K. Raja, and A. J. Kumar, "On the application of a modified self-organizing neural network to estimate stereo disparity," *IEEE Transactions on Image Processing*, vol. 16, no. 11, pp. 2822–2829, 2007.
- [10] K. Sao and B. Yegnanarayana, "Face verification using template matching," *IEEE Transactions on Information Forensics and Security*, vol. 2, no. 3, pp. 636–641, 2007.
- [11] H. C. Lu and C. H. Tsai, "Image recognition study via the neural fuzzy system," *Proceedings of International Conference on Intelligent Engineering Systems*, vol. 6, no. 1, pp. 222–226, 2006.
- [12] Y. Deng, B. S. Manjunath, and H. Shin, "Color image segmentation: proceedings international conference of computer vision and pattern recognition," *IEEE Computer Society Conference*, vol. 2, pp. 446–451, 1999.
- [13] M. Jamshidian and R. I. Jennrich, "Conjugate gradient acceleration of the EM algorithm," *Journal of American Statistical Association*, vol. 88, no. 421, pp. 221–228, 1993.

- [14] D. M. Titterton, A. F. M. Smith, and U. E. Makov, *Statistical Analysis of Finite Mixture Distributions*, John Wiley and Sons, 1985.
- [15] Y. M. Chu, N. A. Shah, P. Agarwal, and J. D. Chung, "Analysis of fractional multi-dimensional NavierStokes equation," *Advances in Difference Equations*, vol. 2021, no. 1, 2021.
- [16] W. He, N. Chen, I. Dassios, N. A. Shah, and J. D. Chung, "Fractional system of Korteweg-De Vries equations via Elzaki transform," *Mathematics*, vol. 9, no. 6, p. 673, 2021.
- [17] N. A. Shah, P. Agarwal, J. D. Chung, E. R. El-Zahar, and Y. S. Hamed, "Analysis of optical solitons for nonlinear Schrödinger equation with detuning term by iterative transform method," *Symmetry*, vol. 12, no. 11, p. 1850, 2020.
- [18] N. A. Shah, I. Dassios, and J. D. Chung, "Numerical investigation of time-fractional equivalent width equations that describe hydromagnetic waves," *Symmetry*, vol. 13, no. 3, p. 418, 2021.
- [19] G. McLachlan and D. Peel, *Finite Mixture Models*, John Wiley and Sons, 2004.
- [20] B. G. Lindsay, *Mixture Models, Theory, Geometry and Applications*, IMS, 1995.
- [21] B. Everitt and D. J. Hand, *Finite Mixture Distributions*, Chapman and Hall, 1981.
- [22] J. D. Foley, *Computer Graphics, Principles and Practice*, Addison-Wesley, 1996.
- [23] R. A. Howard, *Dynamic Probabilistic Systems: Markov Models*, John Wiley and Sons, 2007.
- [24] L. Kotoulas and I. Andreadis, "Colour histogram content-based image retrieval and hardware implementation," *IEE Proceedings, Circuits, Devices and Systems*, vol. 150, no. 5, pp. 1902–1912, 2003.
- [25] H. L. Tang, R. Hanka, and H. H. S. Ip, "Histological image retrieval based on semantic content analysis," *IEEE Transaction on Information Technology in Biomedicine*, vol. 7, no. 1, pp. 26–36, 2003.
- [26] P. T. Yap and R. Paramesran, "Content-based image retrieval using Legendre chromaticity distribution moments," *IEE Proceedings- Vision, Image and Signal Processing*, vol. 153, no. 1, pp. 17–24, 2006.
- [27] Y. D. Khan, F. Ahmad, and S. A. Khan, "Content-based image retrieval using extroverted semantics: a probabilistic approach," *Neural Computing and Applications*, vol. 24, no. 7–8, pp. 1735–1748, 2014.
- [28] W. Jiang, G. Er, Q. Dai, and G. Jinwei, "Similarity based online feature selection in content based image retrieval," *IEEE Transaction on Image Processing*, vol. 15, no. 3, pp. 702–712, 2006.
- [29] K. Wu and K. H. Yap, "Fuzzy SVM for content based image retrieval: a psuedo-label support vector machine framework," *IEEE Computational Intelligence Magazine*, vol. 1, no. 2, pp. 10–16, 2006.
- [30] J. Laaksonen, M. Koskela, S. Laakso, and E. Oja, "PicSOM - content-based image retrieval with self-organizing maps," *Pattern Recognition Letters*, vol. 21, no. 13–14, pp. 1199–1207, 2000.
- [31] N. Marakakis Galatsanos, A. Likas, and A. Stafylopatis, "Probabilistic relevance feedback approach for content-based image retrieval based on Gaussian mixture models," *IET Image Processing*, vol. 3, no. 1, pp. 10–25, 2009.
- [32] F. G. B. Grigorova Natalie, C. Dagli, and T. S. Huang, "Content based image retrieval by feature adaptation and relevance feedback," *IEEE Transaction on Multimedia*, vol. 9, no. 6, pp. 1183–1192, 2007.
- [33] Q. Qiu and L. M. Lam, "Frequency layered color indexing for content based image retrieval," *IEEE Transaction on Image Processing*, vol. 12, no. 1, pp. 102–103, 2003.
- [34] E. A. Castro and D. L. Donoho, "Does median filtering truly preserve edges better than linear filtering," *Annals of Statistics*, vol. 37, no. 3, pp. 1172–1206, 2009.
- [35] G. R. Arce, *Nonlinear Signal Processing: A Statistical Approach*, Wiley, 2004.
- [36] R. Krishnapuram, S. Medasani, S. H. Jung, Y. S. Choi, and R. Balasubramaniam, "Content based image retrieval on a fuzzy approach," *IEEE Transaction on Knowledge and Data Engineering*, vol. 16, no. 10, pp. 115–1199, 2004.
- [37] S. S. Rao, S. Ikram, and P. Ramesh, "Deep learning-based image retrieval system with clustering on attention-based representations," *SN Computer Science*, vol. 2, no. 3, pp. 1–16, 2021.
- [38] P. Singh, P. N. Hrisheeksha, and V. K. Singh, "CBIR-CNN: content-based image retrieval on celebrity data using deep convolution neural network," *Recent Advances in Computer Science and Communications (Formerly: Recent Patents on Computer Science)*, vol. 14, no. 1, pp. 257–272, 2021.
- [39] R. R. Saritha, V. Paul, and P. G. Kumar, "Content based image retrieval using deep learning process," *Cluster Computing*, vol. 22, no. S2, pp. 4187–4200, 2019.
- [40] U. Sharif, Z. Mehmood, T. Mahmood, M. A. Javid, A. Rehman, and T. Saba, "Scene analysis and search using local features and support vector machine for effective content-based image retrieval," *Artificial Intelligence Review*, vol. 52, no. 2, pp. 901–925, 2019.
- [41] A. Tefas, "Deep convolutional learning for content-based image retrieval," *Neurocomputing*, vol. 275, pp. 2467–2478, 2018.
- [42] R. Rahmani, S. A. Goldman, H. Zhang, S. R. Choletti, and J. E. Fritts, "Localized content-based image retrieval," *IEEE Transaction on Pattern Analysis and Machine Intelligence*, vol. 30, no. 11, pp. 1902–1912, 2008.
- [43] R. C. Gonzalez and R. E. Woods, *Digital ImageProcessing*, Pearson Prentice Hall, 3rd edition, 2012.
- [44] P. Pillai, *Probability, Random Variable and Stochastic Processes*, Tata McGraw-Hill Education, 2012.
- [45] S. C. Choi and R. Wette, "Maximum likelihood estimation of the parameters of the gamma distribution and their bias," *Technometrics*, vol. 11, no. 4, pp. 683–690, 1969.
- [46] R. Weber and M. Mlivoncic, "Efficient region-based image retrieval," in *Proceeding CIKM '03 Proceedings of the Twelfth Internationa Conference on Information and Knowledge Management*, pp. 69–76, New York, NY, USA, 2003.
- [47] Y. D. Chun, K. C. Kim, and I. H. Jang, "Content based image retrieval using multiresolution color and texture features," *IEEE Transaction on Multimedia*, vol. 10, no. 6, pp. 1073–1084, 2008.